Molecular Crystals and Liquid Crystals Science and Technology. Section A. Molecular Crystals and Liquid Crystals

Publication details, including instructions for authors and subscription information:
http://www.tandfonline.com/loi/gmcl19

Intermittency at the DSM1-DSM2 Transition in Nematic Liquid Crystal Films

N. Scaramuzza [a] , C. Versace [a] & V. Carbone [a]

[a] Dipartimento di Fisica, Università della Calabria and Consorzio INFM, unità di Cosenza, 87036, Rende (CS), Italy

Version of record first published: 23 Sep 2006.

To cite this article: N. Scaramuzza , C. Versace & V. Carbone (1995): Intermittency at the DSM1-DSM2 Transition in Nematic Liquid Crystal Films, Molecular Crystals and Liquid Crystals Science and Technology. Section A. Molecular Crystals and Liquid Crystals, 266:1, 85-98

To link to this article: http://dx.doi.org/10.1080/10587259508033634

Mol. Cryst. Liq. Cryst. 1995, Vol. 266, pp. 85–98
Reprints available directly from the publisher
Photocopying permitted by license only

Intermittency at the DSM1-DSM2 Transition in Nematic Liquid Crystal Films

N.Scaramuzza ,C.Versace and V.Carbone

Dipartimento di Fisica Università della Calabria and Consorzio INFM, unità di Cosenza, 87036 Rende (CS) Italy

Abstract In this letter we report on the turbulence to turbulence transition, which occurs in a homogeneously oriented nematic liquid crystal (NLC) film under the action of an external alternate voltage. Our observation show that the transition is characterized by a NLC-substrate anchoring breaking, which results in the on set of the twist distortion of the molecular director field. We give the characterization of the different dynamic regimes in terms of the probability distribution functions (PDF's) of the director field curvature energy. The PDF's, which are undoubtedly non-gaussian, indicate that, in both turbulent regimes, the curvature energy is highly intermittent.

Under the effect of a strong external perturbation, many fluid system show a turbulent state[1]; on the contrary, the transition between different turbulent dynamic regimes[2,3] is less common This paper concerns the turbulence to turbulence transition, which take place in a nematic liquid crystal (NLC) film under the action of an external alternating electric field. Figure 1 shows the experimental geometry: the sample cell consists of two square (L ≅ 30x30mm) glass plate spaced by two Mylar strips (d ≅ 50 μm). The cell is filled by capillary flow with the nematic liquid crystal (MBBA). Both the surfaces of the cell are coated by the ACM 72 polymeric surfactant (Atomergic Chemetals Corp.) to induce an homogeneous planar alignment of the unperturbed molecular director $\vec{n}_0$ along the x direction. An alternating voltage is applied crosswise the cell (z direction) by two semitransparent ITO electrodes.

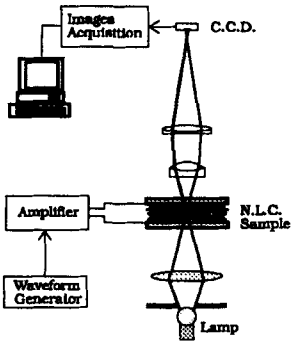

FIGURE 1 Experimental Geometry

The different electroconvective patterns that originate in the NLC cell have been observed by an optical polarizing microscope and the images of sample were acquired by a CCD element connected to a digital image processor. Each two-dimensional image was digitized into 512x512 pixels with a 8 bits resolution (256 gray levels). The frequency ν of the external excitation was fixed at the value of 70Hz, i.e. in the conductive regime[4] (in our cell the cut-off frequency has been found at $\nu_c \approx 200\text{Hz}$. Above a threshold voltage V_1 (in our case $V_1 = 6.8$ Volts r.m.s.) the first electroconvective instability sets up. It consists in a series of stationary parallel straight line (Williams domains) whose periodicity is more or less equal to the cell thickness[5], see picture 1 at the end of the text. This pattern is easily observed if the polarization of the incident light is parallel to $\vec{n}_0$. Indeed, in this condition, the polarization of the incident light is sensitive to the modulation of the refractive index of the sample due to the convective cylindrical rolls, which act as a set of parallel cylindrical lenses and focus the light in series of parallel bright and dark strips on the detector. A small increase of the applied voltage V_0 destabilizes the Williams domains, as shown in picture 2. Then, at higher V_0, we observe a first transition to a weak turbulent state (see picture 3). The transition scenarios can be different depending on the frequency of the external voltage and the presence of defect in the sample. The system can undergo directly to the weak turbulence state or the transition can be preceded by the formation of different spatial static structure: the zigzag undulated rolls structure and the rectangular structure[6,7]. At higher voltage the turbulence completely develops and the so called dynamical scattering mode (DSM) is reached, see picture 4. Above a threshold voltage, while keeping

fixed V_0, a transition between two different kinds of DSM can been observed[3] (the DSM1 and the DSM2 state). This transition is characterized by a transient bimodality of the PDF's of the transmitted light intensity[3], related to different defect density of the two dynamical states. An other important aspect of the transition is that, while the DSM1 and all the different dynamic regimes and spatial static structures that precede the DSM are sensitive to the polarization of the incident light, the DSM2 is polarization independent. The DSM2 nucleates in some zones of the sample and propagates over all the sample by a domino-like mechanism. It has been observed[8] that the number of DSM2 areas and their grown rate exponentially depend on the applied voltage, as it is expected for a nucleation process. As an example, we report three pictures showing the DSM2 domains which nucleate in the sample at three different voltage few second after the field is switched on. The number of DSM2 domains increases with V_0 and, if the sample is observed by linearly polarized incident light, the background DSM1 area shows a different contrast with respect to the DSM2 domains. In particular, if the incident polarization forms an angle of 90° with respect to $\vec{n}_0$, the DSM2 areas can be more easily observed . When, in the DSM2 regime, the field is switched off, a lot of anchoring defects are still visible in the sample. If the sample is observed between crossed polarizers with the incident polarization parallel to $\vec{n}_0$, these defects looks like closed bright lines, roughly circular in shape and their size slowly decreases in time. After a longer time (30÷40 s. for $V_0 \cong 80$ Volts rms.) the disinclination walls disappear and the entire sample relaxes to the undistorted planar alignment. As an example, picture 8 shows the anchoring defects that can be observed in the sample 10 second after V_0 is switched of from 80 Volts rms. These closed disinclination walls indicates surface lines on which the molecular director $\vec{n}(\vec{r})$ has different distortion angle with respect to the anchoring direction $\vec{n}_0$. From the above experimental evidences, we interpret the DSM1-DSM2 transition in terms of an anchoring breaking: During the different dynamic regimes that precede the DSM2 state, since the surface flow velocity is negligible, the molecular director field $\vec{n}_s(\vec{r})$ remains unperturbed at the surface. At the DSM1-DSM2 transition, $\vec{n}_s(\vec{r})$ tilts out from the unperturbed direction and a twist deformation is established.

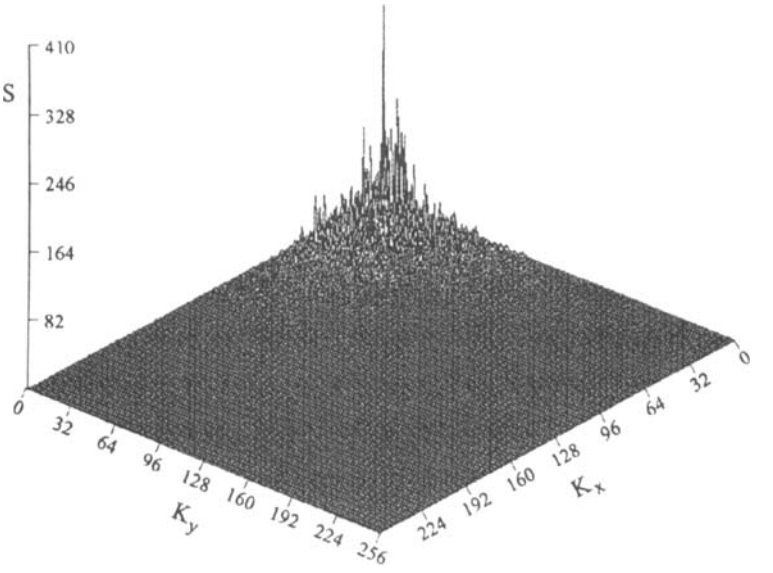

FIGURE 2 Power spectrum S of the weak turbulent regime digitized image, both the maximum x and y wave numbers correspond to 3.07 μm^{-1}.

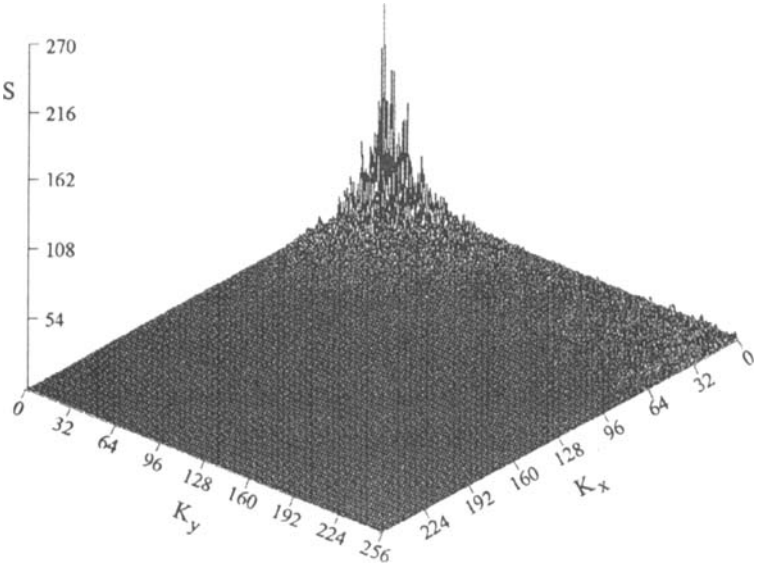

FIGURE 3 Power spectrum S of the DSM1 digitized image, both the maximum x and y wave numbers correspond to 3.07 μm^{-1}.

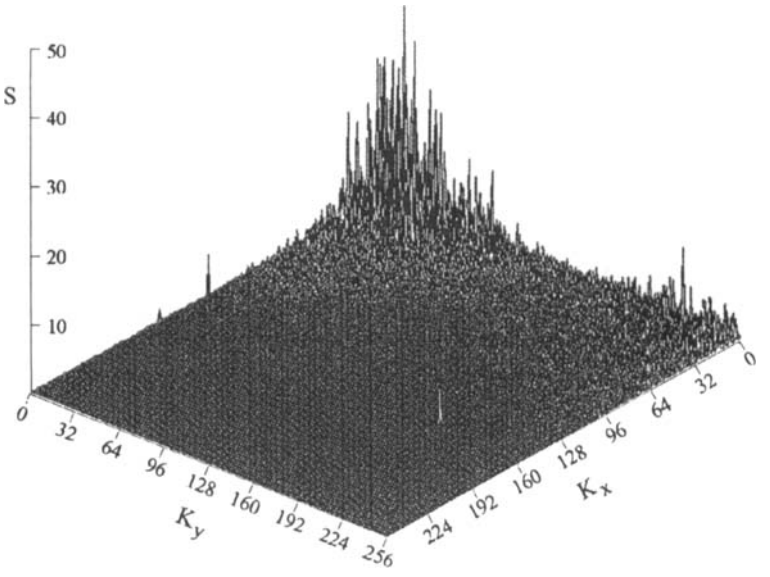

FIGURE 4 Power spectrum S of the DSM2 (85 Volts) digitized image, both the maximum x and y wave numbers correspond to 3.07 μm^{-1}.

In figures 2, 3 and 4 we show the spatial power spectra $S(k_x,k_y)=\left|\frac{1}{4\pi^2 l^2}\int e^{i(k_x\cdot x)}dx\int I(x,y)e^{i(k_y\cdot y)}dy\right|^2$ of the 2D sample images I(x,y) in the weak turbulent state and in both DSM states: figure 3 refers to the DSM1 state (few seconds after the voltage has been applied) figure 4 has been taken 180 seconds later, when the DSM2 has extended over the hole sample. The spectra 3 and 4 show an evident asymmetry. At higher voltage, in fact, both in the DSM1 and DSM2 states, the components with largest wave number (smaller dimension) can grow in the y direction, i. e. perpendicularly to $\vec{n}_0$, but in the DSM2 they are most favored.

This indicate a highest turbulent motion along y, in contrast with the more symmetric weak turbulent spectrum of figure 2. The asymmetry enlarges in the spectrum 4 (DSM2) that shows a greatest high-q contribution.

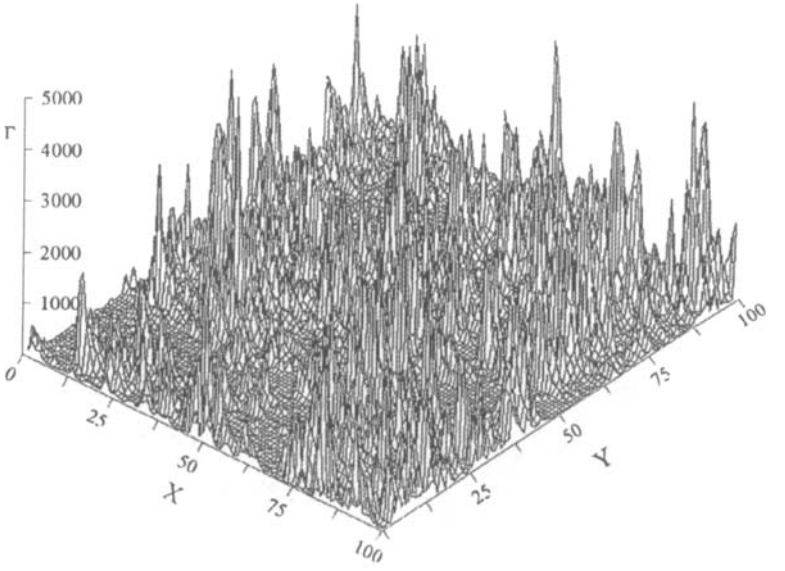

Figure 5: Curvature energy $\Gamma(\vec{r})$ as a function of x and y in the DSM1 regime.

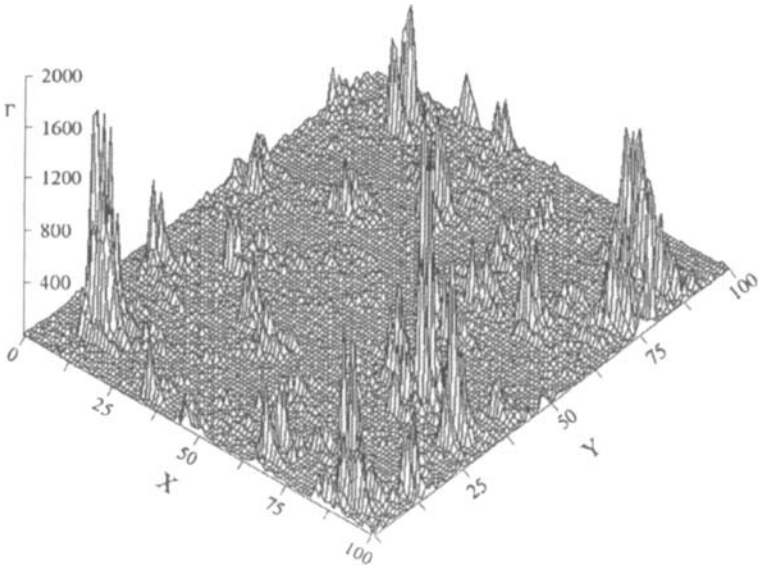

Figure 6: Curvature energy $\Gamma(\vec{r})$ as a function of x and y in the DSM2 regime.

Since the DSM1-DSM2 transition is marked by the onset of a surface deformation, it can be conveniently characterized by the curvature energy of the director field, which is proportional to the quantity $\Gamma(\vec{r}) = \left|\vec{\nabla}[I(\vec{r})]\right|^2$. Of course, only the x and the y components of $\vec{\nabla}[I(\vec{r})]$ are experimentally accessible, but we expect that, if any difference in $\Gamma(\vec{r})$ is observed after the transition, such difference must be imputed to the additional twist deformation that happens in the xy plane. Figures 5 and 6 show the curvature energy $\Gamma(\vec{r})$ calculated over the 100x100 pixel central region of the sample. Both figures refer to V = 85 Volts, figures 5 has been calculated by the image taken 3 s. after V was switched on (DSM1) and figure 6 refers to the situation of the sample after 60 s, when the DSM2 regime has spread over all the sample.

Both Figure 5 and Figure 6 show high $\Gamma(\vec{r})$ peaks which indicates region of the sample where the curvature field is highly singular. This behavior indicates the intermittent character of $\Gamma(\vec{r})$, which is more evident in the DSM2 regime (see Figure 6). The intermittency is better evidenced if we look at the probability distribution functions (PDF's) of $\Gamma(\vec{r})$, which are shown, for three different value of V in the Figure 7 in the DSM1 (A) and DSM2 (B) regimes.

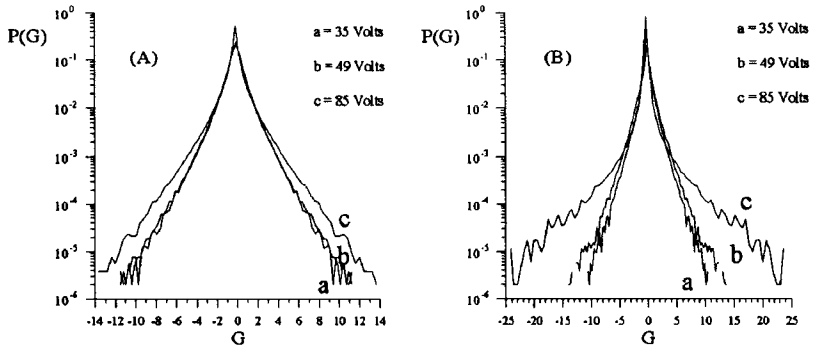

Figure 7 Normalized PDF's of $\Gamma(\vec{r})$ calculated in both the DSM1 (A) and the DSM2 (B).

In both DSM1 and DSM2 regimes the PDF's show a typical exponential tail which indicates that high values of $\Gamma(\vec{r})$ are more probable then in the case of the gaussian PDF and proves the intermittent nature of $\Gamma(\vec{r})$. Furthermore as V increase the tails of the PDF's became more and more important, this tendency is evident both in the DSM1 and DSM2 regimes, but it is more pronounced in the latter regime. The weight of the distribution tail can be quantified by the kurtosis $k = \sum_{i=1}^{N}\left[\frac{\Gamma(\vec{r}_i) - <\Gamma>}{\sigma}\right]^4 - 3$, where N is the number of pixels and σ^2 is the variance of the Γ values distribution, obviously for a Gaussian PDF we have $k = 0$. In Figure 8 we report k as function of applied voltage V (RMS.), as it can be seen k grows more rapidly in the DSM2 regime.

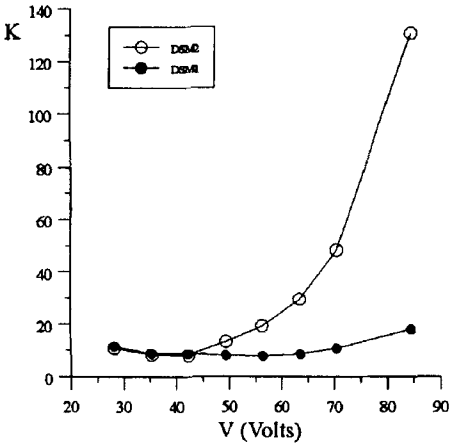

Figure 8 Kurtosis of the $\Gamma(\vec{r})$ PDF's as function of the applied voltage.(RMS.).

In conclusion, our observations contribute to draw a picture of the DSM1-DSM2 transition occurring during the electro hydrodinamic convection in terms of the anchoring breaking of the NLC director on the substrate: the polarization sensitivity that characterizes the Williams rolls as well as both the first weak turbulent regime and the DSM1 regime indicates that the director distortion happens in the plane that contains the unperturbed director $\vec{n}_0$ and the normal $\vec{v}$ to the surfaces (no twist deformation of $\vec{n}(\vec{r})$is allowed).

Near the surface, where the fluid velocity is negligible, the molecular director $\vec{n}_s(\vec{r})$ is still parallel to $\vec{n}_0$. At the DSM1-DSM2 transition, a twist deformation of $\vec{n}(\vec{r})$ rises, even near the surface, starting from several nucleation points, which can coincide with any anchoring defect or disinclination which are present in the cell. In the case of an uniform anchoring, characterized by large zones of the sample without any observable defect, the nucleation points are randomly distributed, indicating the process is activated by any spontaneous fluctuation of $\vec{n}(\vec{r})$. Afterwards, the deformation propagates over all the sample by an absorption effect to complete the transition. At present, about the origin of the surface deformation we are able only to give a qualitative interpretation. As our analysis shows, the intermittence of the distortion energy density $\Gamma(\vec{r})$ increases along with the external applied voltage V. This means that, as V increases the disinclination electro-convective loops become smaller and smaller. This process gives rise to a large order parameter variation between the bulk and the surface of the sample, which cause a large ordoelectric polarization[9]. Following Ref.10, an anchoring transition, due to the order electric effect, can be predicted. As the order parameter difference ΔS among the bulk and the surface of the sample exceeds a threshold values, $\vec{n}_s(\vec{r})$ tilts and the turbulence reaches the surface. In this frame we can also explain the increasing of the DSM1-DSM2 threshold which we have observed in weak anchored cell. In fact, in the latter case, since the order induced by the substrate is reduced, ΔS and, as a consequence, the ordoelectrictic polarization, which one can obtain at a given applied voltage, are smaller; thus a higher voltage is required to set up the DSM2 regime. This interpretation conflicts with the microscopic treatment of the nematic order. Indeed S is defined on the nematic molecular correlation length ξ that is few hundred Angstrom, which is well below the hydrodynamic scale. This means that, to give any quantitative description of the phenomenon all the microscopic quantities related to the nematic order have to be scaled to the hydrodynamic scale. However, the higher intermittency we have found in the DSM2 indicates that, in this dynamic regime, the NLC flow can reach smaller scales, so the order of the system, even though on a hydrodynamic scale decreases.

The authors would like to thank Prof. A.G.Petrov, Prof. G. Barbero and Prof. R.Ribotta for stimulating discussions.

REFERENCES

1. D.C. Leslie Developments in the theory of turbulence (Oxford University Press, London 1973)
2. R.P. Behringer, Review of Modern Physics 57, 657 (1985)
3. S.Kai, M.Andoh, S.Yamaguchi Physical Review A 46, 7375 (1992)
4. P.G. de Gennes The Physics of Liquid Crystals (Oxford University Press London 1975)
5. R.Williams Journal of Chemical Physics 39, 384 (1963)
6. A.Joets, R.Ribotta Journal de Physique 47, 595 (1986)
7. S.Nasuno, O.Sasaki, S. Kai Physical Review A 46 4954 (1991)
8 S.Kai, W.Zimmermann, M.Andoh, N.Chizumi Physical Review Letters 64, 1111 (1990)
9. G.Barbero, I.Dozov, J.F.Palierne, G.Durand Physical Review Letters 56, 19 (1986)
10. G.Barbero, A.G.Petrov Journal of Physics: Condensed Matter 6, 2291 (1994)

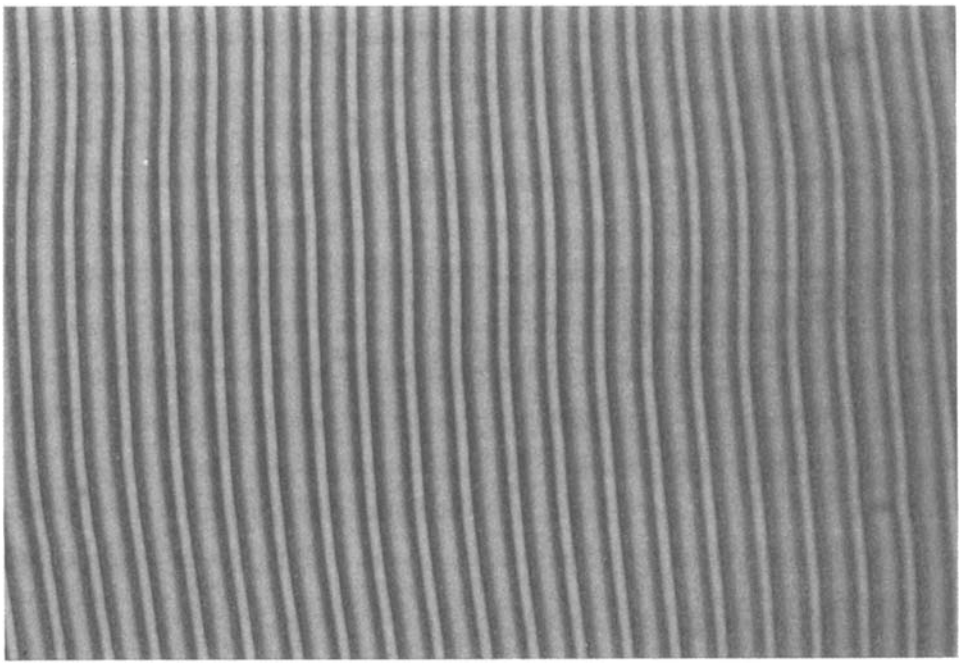

Picture 1 The Williams rolls, V_{rms}= 6.8 Volts, 150 times magnifications, the polarization of the incident light is along $\vec{n}_0$. See Color Plate III.

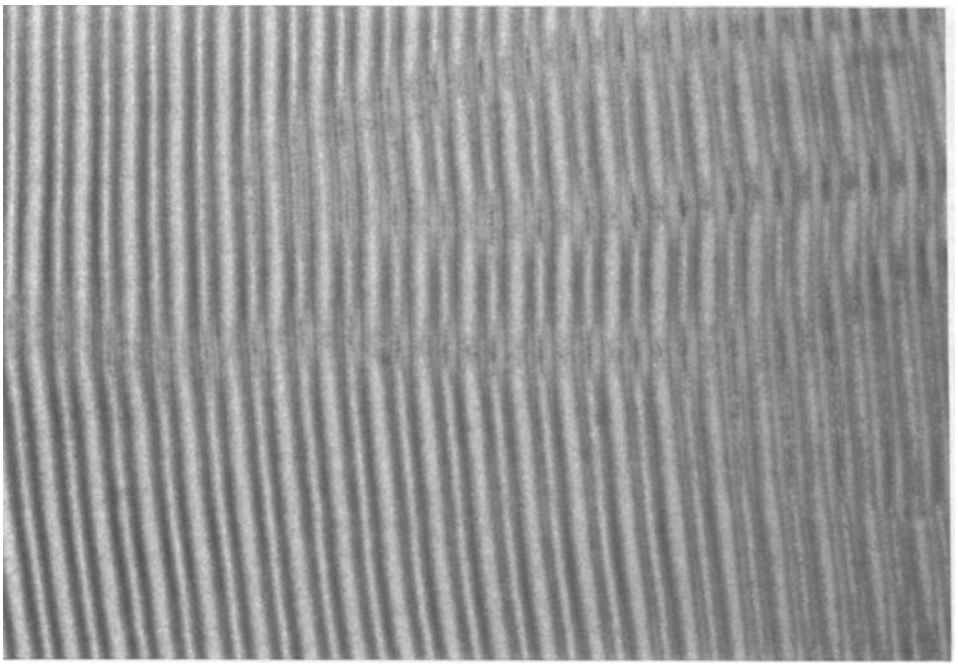

Picture 2 The distorted Williams rolls, V_{rms}= 7.1 Volts, 150 times magnifications, the polarization of the incident light is along $\vec{n}_0$. See Color Plate IV.

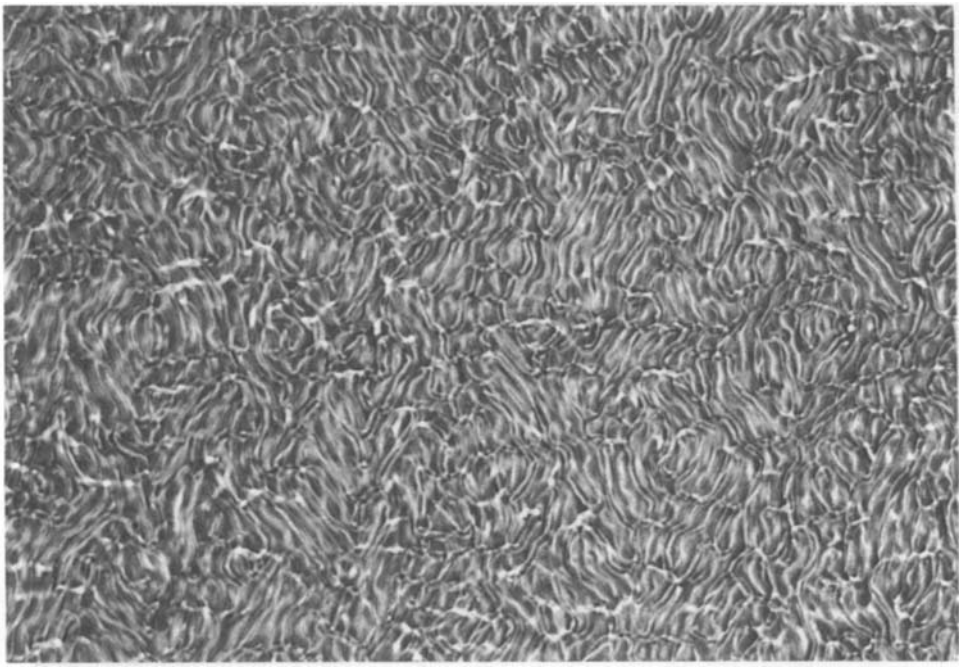

Picture 3 The weak turbulent state, V_{rms}= 14.5 Volts, 37 times magnifications, the polarization of the incident light is along $\vec{n}_0$. See Color Plate V.

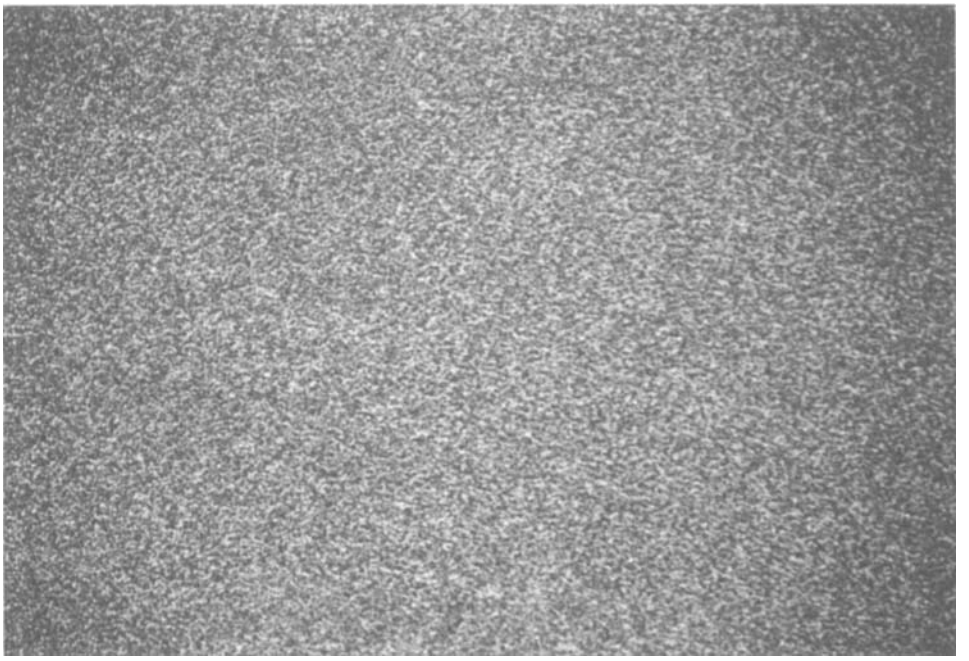

Picture 4 The DSM1 state, V_{rms}= 40 Volts, 37 times magnifications, the polarization of the incident light is along $\vec{n}_0$. See Color Plate VI.

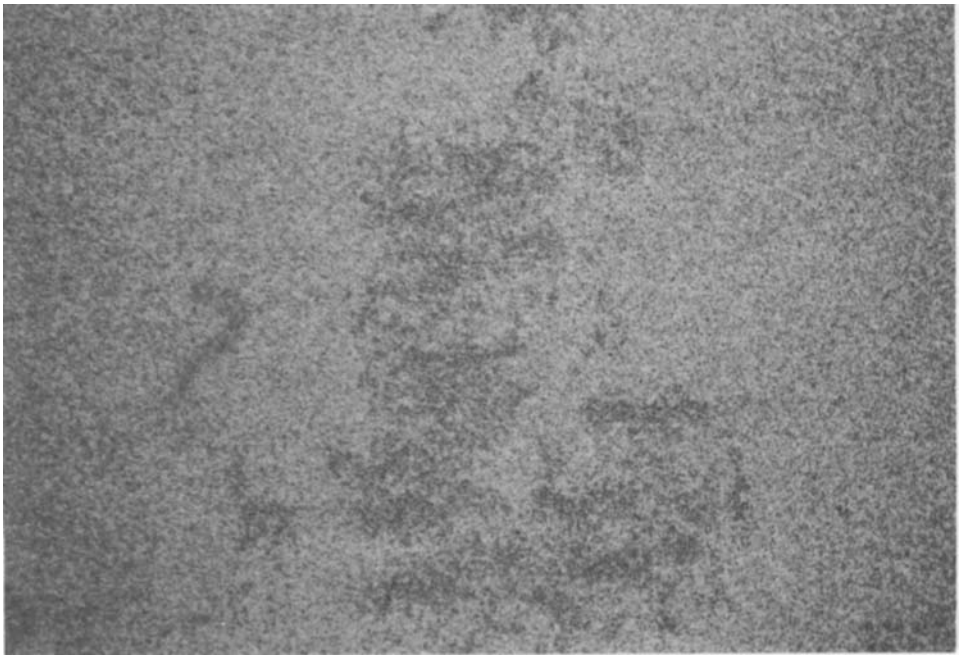

Picture 5 The DSM1 state along with some DSM2 nucleating areas, V_{rms}= 30 Volts, 37 times magnifications, the polarization of incident light is normal to $\vec{n}_0$.
See Color Plate VII.

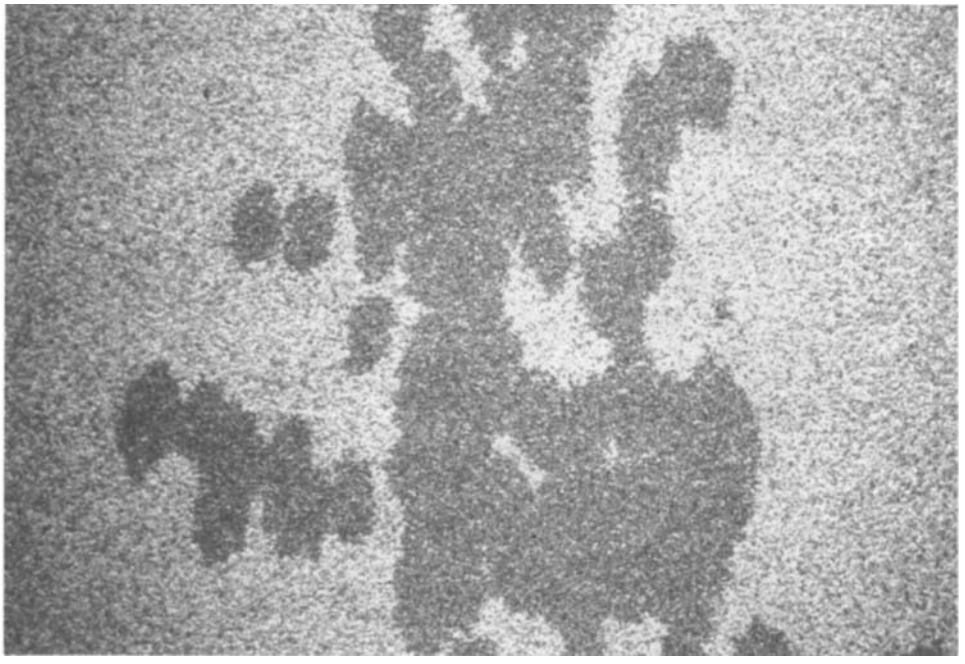

Picture 6 The same as picture 5, V_{rms}= 50 Volts. See Color Plate VIII.

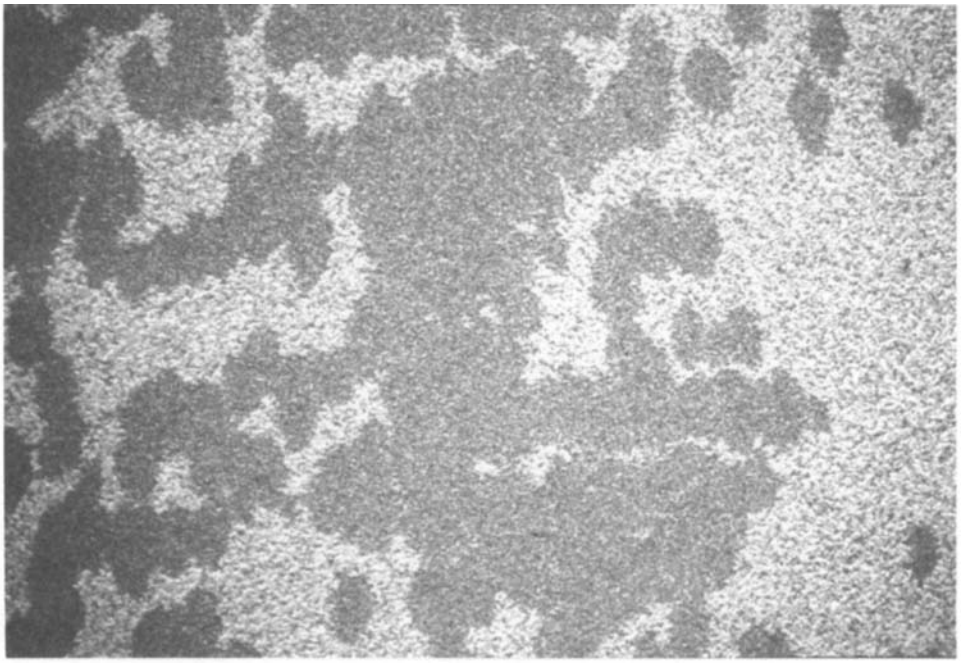

Picture 7 The same as picture 5, V_{rms}= 80 Volts. See Color Plate IX.

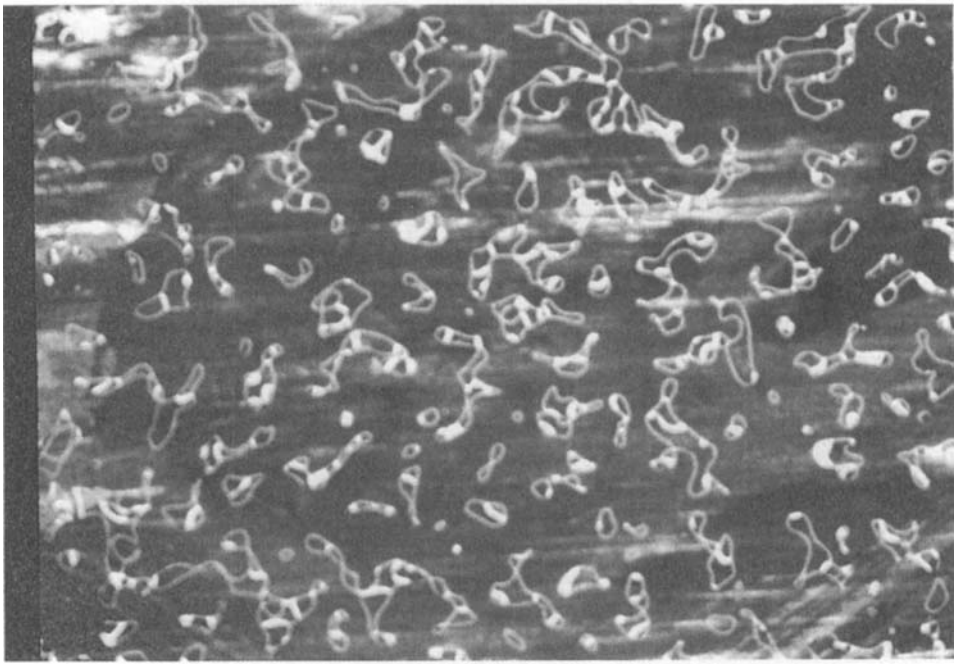

Picture 8 Defects still present in the sample 10 s. after the applied voltage is switched off from V_{rms}= 80 Volts, 37 times magnification, the polarization of the incident light is normal to $\vec{n}_0$, crossed analyser **See Color Plate X.**